# Model-Assisted Probability of Detection of Cracks Under Fastener Head

YOUNGCHAN KIM, SEONHWA JUNG and DOOYOUL LEE

## ABSTRACT

After the Aloha Airlines Flight 243 accident in 1988, the importance of inspecting for widespread fatigue damage was emphasized. Managing the risk of multi-site damage (MSD), where multiple flaws occur in a single structure, became a key factor in maintaining the structural safety of aircraft. It is essential to demonstrate the reliability of nondestructive inspection (NDI) when detecting structural damage due to MSD. Structures affected by MSD often require inspection without being disassembled due to various reasons, such as increased inspection time, inefficient manpower and material consumption, and increased probability of MSD due to human error. NDI reliability is strongly influenced by the shape of the test specimen, and the uncertainty about crack conditions after inspection is greater when inspection is performed on a structure without disassembly than when it is assembled. To estimate the reliability of NDI in structures without disassembly, a model-assisted probability of detection (MAPOD) experimental design was used, combining physical modeling and machine learning methods. The test specimens simulated flaws such as discharge machining notches and fatigue cracks, and the detection probability was estimated based on the size of the detection signal. This was used in risk assessment to determine the inspection interval for the structure.

## INTRODUCTION

Nondestructive inspection (NDI) reliability is evaluated as the probability of detecting defects in aircraft structures based on their size and plays a significant role in determining appropriate inspection methods and intervals.[1]–[4] However, it is difficult to obtain an amount of data sufficiently through experimental approaches using specimens and actual flawed products. To overcome this disadvantage, simulation programs with the ability to generate large amounts of relatively inexpensive data have been developed to complement the costly and time-consuming experimental approach. However, there is

---

Youngchan Kim, Seonhwa Jung and Dooyoul Lee, Korea National Defense University, 1040 Hwangsanbul-ro, Yangchon-myeon, Nonsan-si, 33021 Chungcheongnam-do, Korea

a high level of uncertainty in evaluating NDI capabilities solely through simulation. To address this issue, model-assisted probability of detection (MAPOD) is widely used, which utilizes actual data and simulation for insufficient data.[5]–[9]

This study evaluated the NDI capability of operational maintenance personnel without removing fasteners. Performing NDI without removing fasteners can improve efficiency and cost-effectiveness, as the removal of fasteners can result in time and cost, and potential damage to adjacent areas during the removal process. However, the increase in inspection uncertainty is unavoidable due to the presence of fasteners. Thus, experiments were conducted to test the detection probability of operational maintenance personnel using a specimen that simulated the presence of fasteners. Since physical experiments cannot be performed under all conditions, the MAPOD approach was utilized based on a few physical experiments, many simulations, and a transfer function to introduce the uncertainty in the POD curve.[10]

# EXPERIMENTAL

## Specimen

The target of this study was to simulate the Splice Fitting, one of the major structures of the F-15K aircraft as shown in Figure 1.

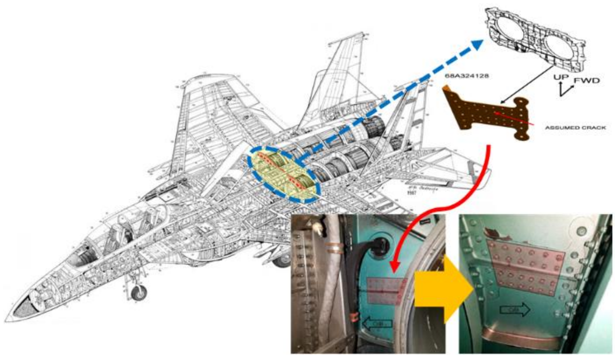


Figure 1 F-15K splice fitting

As shown in Figure 2, the hole size is 4.76mm, and the diameter of the Fastener head is 7.75mm. The length of the crack hidden by the fastener head is 1.5mm. The material of the specimen is Ti-4Al-6V Plate, and the Fastener is PH13-8.[11]

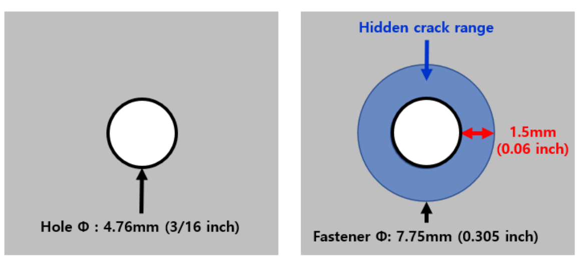


(a) (b)

Figure 2 Schematics of fastener hole (a) without fastener and (b) with fastener

To simulate the Splice Fitting, a specimen was fabricated with the same thickness and hole spacing as the actual component, including the distance between holes and between the holes and ends. The specimen is shown in Figure 3, and six types of artificial cracks ranging from 0.5 mm to 3.0 mm in four directions (0°, 90°, 180°, 270°) were machined using electrical discharge machining (EDM) on 30 of the 45 holes randomly. The remaining 15 holes were left to measure the level of noise. To simulate the fastener, a structure with the same diameter as the actual fastener head was 3D-printed and installed.

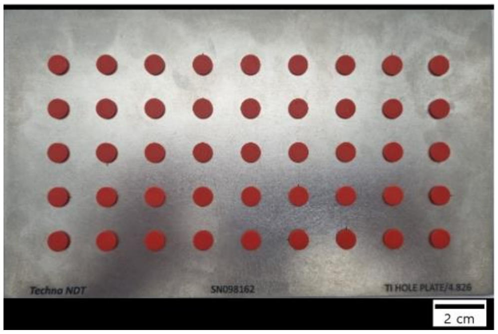

Figure 3 Upper surface of specimen with simulated fasteners

To calibrate the signal amplitudes from simulated cracks using EDM, actual fatigue crack specimens were fabricated. The fatigue cracks were generated by creating a small notch using EDM on a hole, generating fatigue cracks through fatigue testing, and removing the EDM notch part by drilling. Fasteners were then fastened to the specimen.

## Eddy current inspection (ECI) experiment

The ECI was performed according to T.O 33B-1-1 using Staveley Nortec 600D equipment.[12] A frequency of 1 MHz is used to test Ti-6Al-4V, which requires a high frequency. The probe used was a right-angle type, and the coil type is an absolute bridge. According to the maintenance manual of the aircraft operated by the ROAKF, a signal detection of 10–20% of full screen height (FSH) or higher is considered a defect. Therefore, the noise is set to 10% of FSH, and the inspectors' defect determination criteria are set to 15% of FSH for analysis.

## ECI simulation

ECI was simulated using CIVA software to obtain signal amplitudes according to the size of defects on a Ti-4V-6Al plate.[13] The main parameters are sample's flaw length, lift–off, frequency and conductivity. Simulation were conducted under conditions such as in a physical experiment.

## MAPOD

The POD methodology is described in US DoD Handbook 1823A[4], and parameter estimation follows the Berens model adopted by ASTM standards.[14] The Berens model, introduced in 1988, is defined based on the measurement signal a as follows.

$$\hat{a}(a) = \hat{\beta}_0 + \hat{\beta}_1 a + \varepsilon \quad (1)$$

where $\hat{\beta}_0$ and $\hat{\beta}_1$ are parameters of the linear model, and e is the model error. $\hat{\beta}_0$, $\hat{\beta}_1$, and $\hat{a}_\varepsilon$ are estimated using the maximum likelihood estimation. As the simulation results show a difference from the results of the physical experiments, the simulation results are adjusted through the physical experiments. Both simulation and physical experiments have the independent variable of the fault size (a) and the dependent variable of the measured signal size ($\hat{a}$), which are transformed appropriately to show a linear relationship. First, the linear relationship obtained from the physical experiment is as follows.

$$y = \beta_{0e} + \beta_{1e} x_e \quad (2)$$

where $\beta_{1e}$ and $\beta_{0e}$ represent the slope and y-intercept of the linear regression equation obtained from the simulation, respectively. Similarly, the linear regression equation obtained from the simulation can be expressed as follows.

$$y_s = \beta_{0s} + \beta_{1s} x_s \quad (3)$$

where $\beta_{1s}$ and $\beta_{0s}$ represent the slope and y-intercept of the linear relationship obtained from the simulation, respectively. The transfer function used to correct the response signal from the simulation can be obtained using the linear relationships in Eq. (2) and Eq. (3), as shown in Eq. (4).[10]

$$F(a) = \frac{\beta_{0e} + \beta_{1e} a}{\beta_{0s} + \beta_{1s} a} \quad (4)$$

The transfer function in Eq. (4) estimates the response of a complex target from the response of a simple target. Therefore, even with a small number of physical experiments, it can help derive relevant conclusions through statistical analysis. The method of obtaining the corrected response signal by multiplying this transfer function with the response signal from the simulation is shown in Eq. (5).

$$\text{Transferred defect response} = \text{Simulated defect response} \times F(a) \quad (5)$$

## RESULTS AND DISCUSSION

### Descriptive statistics

The results of ECI for EDM notched specimens and actual fatigue crack specimens showed a correlation between the signal amplitude and the size of the crack. The correlation between the signal amplitude measured from EDM notches and actual fatigue cracks showed that the signal amplitude from actual fatigue cracks was about 5-10% lower than that from EDM notches for the same crack size of 3 mm or less.

The $a_{90/95}$ of EDM notch among 5 inspectors lie adjacent to 2.2 mm, while the $a_{90/95}$ of actual fatigue crack specimens is about 2.3 mm, indicating a high probability of detection for crack sizes of 2.3mm or greater.

## Sensitivity analysis

To identify the major factors used for physical experiments, simulations were conducted under various experimental conditions using the non-destructive testing software CIVA. Sensitivity analysis was performed by setting the crack size from 0.25 mm to 8 mm at intervals of 0.25 mm with three other factors (Table. 1) that affect non-destructive testing.[6], [7], [15]

Table. 1 Ranges of parameters for sensitivity analysis

| Parameter | range | Distribution |
|---|---|---|
| Flaw length | 0.25–8 mm | Interval: 0.25 mm |
| Lift-off | 0.04–0.08 mm | Uniform |
| Frequency | 999–1001 MHz | Normal |
| Conductivity | 0.7–0.78 | Normal |

The signal strength of NDI equipment increases with the size of cracks. Therefore, crack size can be estimated by the signal strength. Sensitivity analysis showed that changes in crack size have the greatest impact on signal variation, while the variable of lift-off, which is controlled by the inspector, had the least impact. Therefore, in the physical experiment, variations were assumed to be caused only by changes in crack length, while other variables were fixed. The effects of other variables are reflected through simulations.

## POD curves using signals from EDM notches and fatigue cracks

Before calculating the detectable crack length, the POD curve was obtained by analyzing the ECI signals of individual inspectors. The POD curve for each inspector can be obtained by estimating the parameters of the detection probability model after deriving a linear model between the signal amplitude and crack length. The relationship between the size of the EDM notch in the specimen and the signal amplitude for the five inspectors involved in this study is shown in Figure 4. There is a correlation between the size of the EDM notch in the specimen and the signal size, as Figure 4 shows that the signal size increases with the size of the EDM notches.

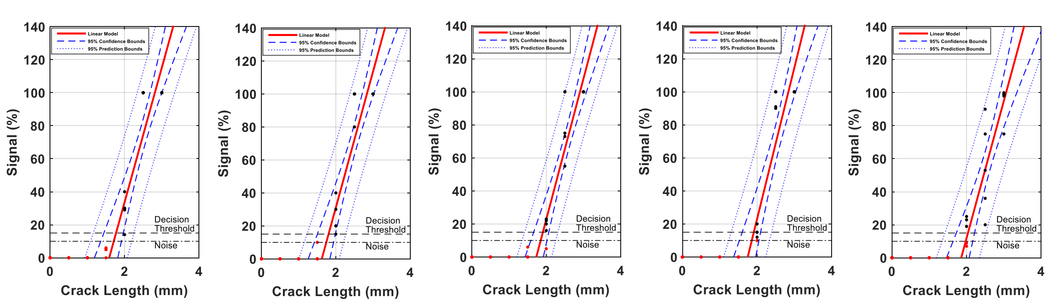


(a) (b) (c) (d) (e)

Figure 4 Signal amplitudes from EDM notches by inspector (a) to (e)

After testing the EDM notch specimens, PODs were obtained for each inspector, as shown in Figure 5. It is assumed that surface cracks can be detected at a size of 1.27 mm. It was predicted that cracks of fastener heads with a size of 2.7–2.8 mm could be detected. However, this study showed that cracks as small as 2.2–2.3 mm could be detected. In the near future, the POD without fastener installation will be analyzed and compared.

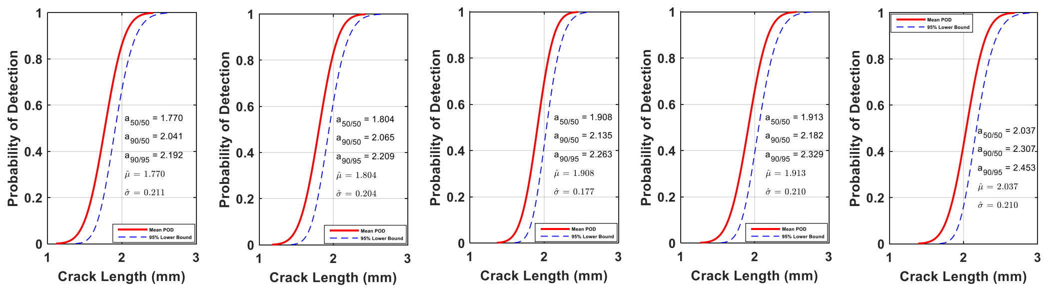


(a) (b) (c) (d) (e)

Figure 5 POD curves using signal amplitudes from EDM notches for inspector (a) to (e)

According to the results of the inspection using a fatigue crack specimen, as shown in Figure 8, the POD for each inspector was derived. Like the EDM notch specimen, fatigue cracks can be detected from the level of 0.5–0.8 mm, but the interval of the crack size in the specimen is 0.5 mm and the quantity is insufficient, resulting in an almost straight-line analysis as shown in Figures 6 (c), (d), and (e).

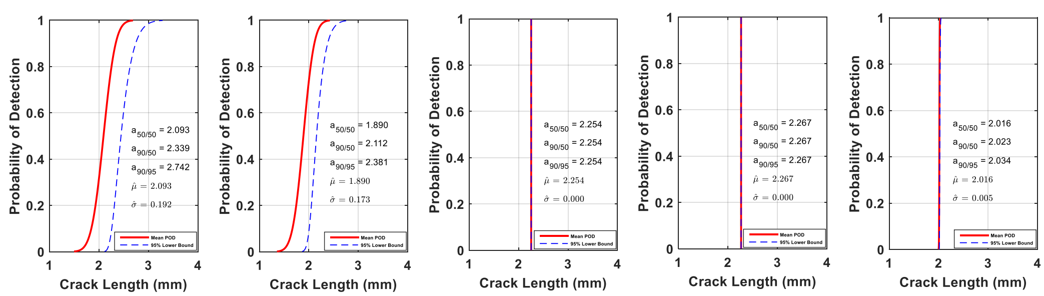


(a) (b) (c) (d) (e)

Figure 6 POD curves using signal amplitudes from fatigue cracks for inspector (a) to (e)

Simulation results using various variables and multiple experimental data to increase the reliability of the POD results are shown in Figure 7. To supplement the insufficient amount of experimentation and data, simulations were conducted by inputting multiple variables.

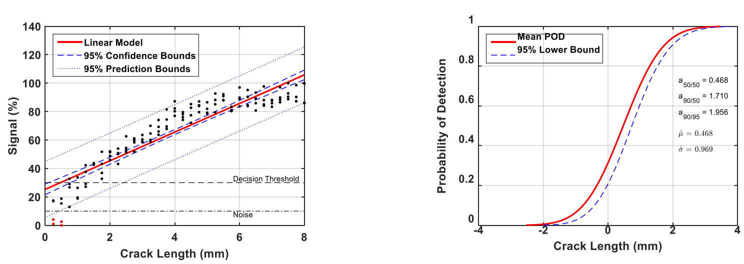


(a) (b)

Figure 7 (a) Signal amplitudes and (b) POD curves obtained using simulation results

Using simulation results and signal amplitudes obtained from EDM Notch and fatigue crack specimens, the final POD for each inspector was obtained using the transfer function in Eq. (4) and is shown in Figure 8. The $a_{90/95}$ for each inspector was found to be an average of 2.3mm when fasteners were present. The blue line in Figure 8 represents the results from the inspection of the fatigue crack specimen, while the red line represents the simulation results incorporating three factors. The MAPOD results using the transfer function are shown in green. The experimental crack sizes and signal amplitudes are averaged, and the simulation results are used to calculate the variance in POD, which can increase the reliability of POD and reduce the cost and time required to obtain experimental data.

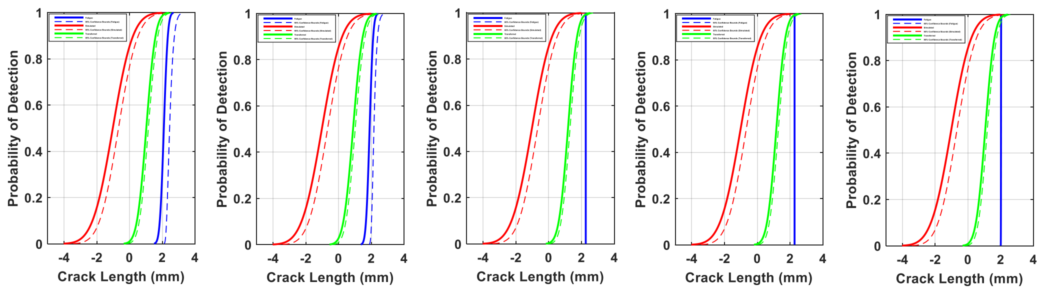


(a) (b) (c) (d) (e)

Figure 8 POD curves using MAPOD for inspector (a) to (e)

## CONCLUSION

Using physical modeling and machine learning methods, the MAPOD experiment plan was developed, resulting in a significant reduction in experimental factors and a reduction in the time and cost required for actual experiments. Simulation was also used to model various factors, increasing not only the reliability of POD but also saving time and cost. This study allows for the quantitative measurement of POD for operating groups in the presence of fasteners, which can be applied to aircraft maintenance plans. Firstly, it can effectively reduce human errors and maintenance time that may occur during fastener removal. Furthermore, in cases where new fasteners must be used when removing fasteners, unnecessary consumption of fasteners can be reduced, resulting in increased economic efficiency for operating groups. Finally, by using POD in the presence of fasteners, the distribution of crack lengths during inspection can be predicted. This allows for risk assessments to be carried out by operating groups to maintain structural safety of the aircraft, and quantitative risk assessments can be used as the basis for decision-making by command staff. This study is expected to have diverse applications, including inspection methods, timing, and structural safety maintenance, and is expected to improve aircraft operation as well as reduce maintenance time and costs while maintaining aircraft structural safety.

## REFERENCES


1. U.S. Department of Defense, "Standard Practice Aircraft Structural Integrity Program (ASIP)," *MIL-STD-1530D*, Change 1., Washington, D.C, (2016).
2. C. Mueller, M. Bertovic, M. Pavlovic, D. Kanzler, U. Ewert., J. Pitkänen and U. Ronneteg, "Paradigm Shift in the Holistic Evaluation of the Reliability of NDE Systems," *Journal of the Materials Testing* 55, no. 4, (2013), pp: 261–269,
3. R. Holstein, M. Bertovic, D. Kanzler, and C. Müller, "NDT Reliability in the Organizational Context of Service Inspection Companies," *Journal of the Materials Testing* 56, no. 7–8, (2014), pp: 607–610
4. U.S. Department of Defense, "Nondestructive Evaluation System Reliability Assessment," MIL-HDBK-1823A, Washington, D.C, (2009).
5. N. Dominguez, F. Reverdy, and F. Jenson, "POD Evaluation using Simulation: A Phased Array UT case on a Complex Geometry Part," Paper presented at the AIP Conference Proceedings, (2014).
6. F. Jenson, H. Ammari, A. Rouhan, N.Dominguez, F. Foucher, A. Le Brun, and J. Moysan., "The SISTAE Project: Simulation and Statistics for Non Destructive Evaluation," Paper presented at the 4th European-American Workshop on Reliability of NDE, (2009)
7. P. Calmon, F. Jenson, and C. Reboud, "Simulated Probability of Detection Maps in case of Non-Monotonic EC Signal Response," Paper presented at the AIP Conference Proceedings, (2015).
8. M. Li, W. Meeker, and R. Thompson, "Physical Model Assisted Probability of Detection in Nondestructive Evaluation for Detecting of Flaws in Titanium Forgings," *Journal of the Aerospace Engineering*, no. 2, (2011), pp: 1–35,
9. F. Foucher, R. Fernandez, S. Leberre, and P. Calmon, "New Tools in CIVA for Model Assisted Probability of Detection (MAPOD) to support NDE Reliability Studies," Paper presented at the Nondestructive Evaluation of Aerospace Materials & Structures Conference Proceedings, (2018).
10. D. Lee, S. Yoon, J. Park, S. Eum, and H. Cho. "Demonstration of Model-Assisted Probability of Detection Framework for Ultrasonic Inspection of Cracks in Compressor Blades," *NDT&E International* 128, (2022).
11. Boeing F-15 ASIP Team, "ROKAF IAT78 Risk Assessment," Boeing Defense, Space & Security, St. Louis, MO, (2021).
12. U.S Air Force Life Cycle Management Center. "NDT General Procedures and Process Controls," *T.O. 33B-1-1*, Wright-Patterson AFB in Dayton, OH, (2007).
13. EXTENDE, "CIVA NDE 2016 Simulation Program User Manual," Massy, France(2016).
14. ASTM International, "Standard Practice for Probability of Detection Analysis for Hit / Miss Data," *E3023-21*, West Conshohocken, PA, (2012), pp: 1–6.
15. R. Jarvis, P. Cawley, and P. B. Nagy, "Performance Evaluation of a Magnetic Field Measurement NDE Technique using a Model Assisted Probability of Detection Framework," *Journal of the NDT&E International* 91, no. 6, (2017), pp: 61–70.